

Crystallization of Membrane Proteins: Merohedral Twinning of Crystals

V. Borshchevskiy^{2,3} and V. Gordeliy^{1,2,3}

¹Laboratoire des Protéines Membranaires,
Institut de Biologie Structurale J.-P.,

²Research-educational Centre "Bionanophysics",
Moscow Institute of Physics and Technology,

³Institute of Complex Systems (ICS),
ICS-5: Molecular Biophysics, Research Centre Juelich,

¹France

²Russia

³Germany

1. Introduction

Membrane proteins are the main functional units of biological membranes. They represent roughly one-third of the proteins encoded in the genome and about 70% of drugs are targeted to membrane proteins. X-ray protein crystallography is one of the most powerful tools to determine protein structure and to provide a basis for understanding molecular mechanisms of protein function. Despite an obvious importance of membrane protein only about 1% of structures in the Protein Data Bank (PDB) are of this type. Moreover, although the number of membrane protein structures deposited to PDB since 1985, date of the first membrane protein structure [1], is increasing it is not yet comparable with the rate achieved for soluble proteins [2]. Currently, the PDB contains more than 70,000 structures, and the structures of membrane proteins do not exceed 500 [3]. Considerable effort made in several laboratories in the last years towards extension of high-throughput crystallography to membrane proteins open a hope of correcting this imbalance. Nevertheless significant challenges must be overcome to achieve this goal. Two major problems toward the determination of membrane proteins structures are: the production of pure, stable and functional protein solubilized in detergents, and the growth of crystals suitable for X-ray crystallography. The latter is often defined as major bottleneck of structural biology of membrane proteins. For a long time, the vapor diffusion method has been the only method which was used to crystallize membrane proteins. This method, which is based on a well-developed approach of crystallization of water soluble proteins, led to relative success, however, it failed to produce crystals of some important membrane proteins. Quite recently new methods were introduced. One of the most promising new method to overcome this problem is the so called *in meso* crystallization approach where lipid systems (e.g. the lipid cubic phase (LCP)) are used as a crystallization matrix. It has been demonstrated that these methods are applicable to different membrane proteins including G-protein-coupled receptors (GPCR), membrane protein complexes and others. One of the first important breakthroughs was bacteriorhodopsin (bR) which for a long time failed to be

crystallized by the *in surfo* methods and was solved to resolution about 1.55 Å from the crystals obtained by LCP crystallization. Thanks to the *in meso* method crystallographic structures of almost all functional states of bR are now available with atomic resolution (see [4] for review). Despite this fact the detailed mechanism of bR proton pumping is still to be elucidated. It appeared that a severe problem originates from the tendency of the best (in the sense of resolution) bR crystals to be perfectly twinned. Being a general problem of protein crystallography, twinning may result in controversial structural models of intermediate states in the case of bR. The chapter presented here is aimed to summarize the present knowledge on twinning formation during *in meso* crystallization and the methods to overcome it.

2. *In meso* crystallization

2.1 Crystallization from lipidic cubic phase

A principally new crystallization method – crystallization of membrane proteins in lipidic cubic phases was developed by Rosenbusch and Landau in 1996 [5]. A fundamental difference between methods of standard crystallization and crystallization in the LCP is that in the latter, the solubilized protein is reconstituted back in the native lipid bilayer and after that the crystallization is induced by the addition of a precipitant. Liquid crystalline systems formed by lipids in aqueous media can form infinite bicontinuous periodic minimal surfaces, which have a zero mean curvature and a periodicity in all the three dimensions characterized by a cubic lattice [6-8]. The system consists of two compartments: a continuous curved lipid bilayer forming a three-dimensional well-ordered structure, interwoven with continuous aqueous channels. Macroscopically the phase is very viscous, isotropic, and optically transparent. Membrane cubic phases are found in the cells [9], and they are used in food industry [10] as well as for drug delivery [11]. Practical aspects of crystallization in the lipidic cubic phase look very simple and an example – crystallization of bR – can be described as the following procedure [12]:

1. Weigh into the PCR tube (200 mL) approximately 5 mg of dry MO, incubate tubes with monooleoyl (MO) at 40°C, and spin the lipid down for 10 min at 13,000 × g at room temperature.
2. Keep MO at 40°C during an additional 20 min to gain the isotropic fluid lipidic phase and then let the lipid phase cool to room temperature.
3. Mix 1 mL of prepared 10 mg/mL BR solution comprising about 1.2 w/w% of *n*-octyl-β-D-glucopyranoside (OG) with 1 mg of MO. To gain the cubic phase, centrifuge the PCR tubes with the sample at 10,000 rpm for at least 1 h at 22°C (rotating tubes within the rotor every 15 min by 90°). Incubate the samples during 1-2 days in the dark at 20-22°C. An alternative way to prepare the cubic phase is described in [13].
4. Add a precipitant to induce crystallization– a ground powder of KH₂PO₄ mixed with Na₂HPO₄ (95/5 w/w) with a final concentration of the salt mixture 1–2.5 M (pH 5.6). Repeat homogenizing centrifugation of samples as described in the previous item. Leave the crystallization batch in the dark at 22°C. bR microcrystals (10–20 μm in diameter) usually appear within 1 week after induction of crystallization (Fig. 1). This protocol of crystallization is close to the original one provided by Rosenbusch and Landau. An alternative way to do such crystallization (it is used in nanovolume high throughput approach) is to add liquid precipitant to the top of the lipidic phase [13].
5. To separate the crystals from the lipidic phase directly from LCP use mechanical manipulation with microtools or, alternatively, add lipase or detergent to the lipidic phase to destroy the lipid phase at room temperature during several hours or days [14].

LCP approach remains most efficient among all other *in meso* approaches introduced later. Nevertheless, it is not yet clear whether other new methods were properly optimized. In other words it is not yet clear what is the real potential of these methods. Therefore, we will describe briefly three more new approaches

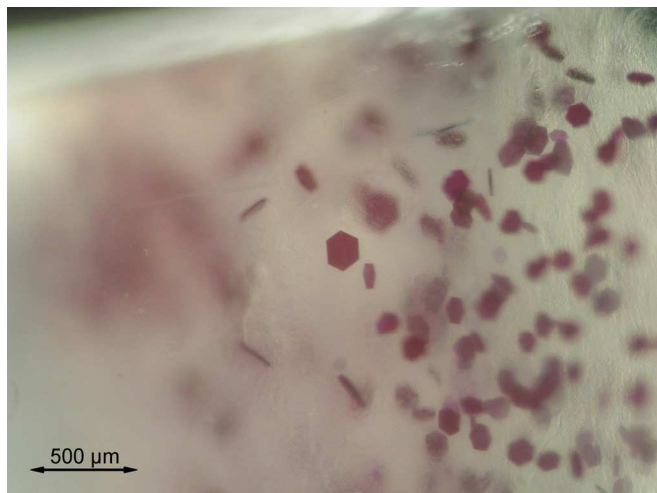


Fig. 1. A crystallization well (a PCR tube) with bR crystals.

2.2 Crystallization from vesicles

An interesting and unusual approach to membrane protein crystallization was proposed in 1998 [15,16]. The authors observed that purple membranes (two-dimensional hexagonal native crystals of bR) treated with the neutral detergent under certain conditions lead to the creation of spherical protein clusters (~50 nm in diameter). Using a standard vapor diffusion method for crystallization from bR vesicles with a high protein/lipid ratio, well diffracting hexagonal crystals were obtained [15-17]. This new crystal belongs to the space group $P622$ with unit cell dimensions of $a = b = 104.7 \text{ \AA}$ and $c = 114.1 \text{ \AA}$. The highest announced structural resolution achieved by this method is 2.0 \AA . It is not compared to the LCP results obtained with the same protein. Until now there is no evidence that a specific case of bR crystallization from vesicles can be extended to other membrane proteins. However, it is not yet clear whether this approach is limited to some specific cases, like bR, or has a more general application.

2.3 Crystallization from bicelles

Just after the second *in meso* method was published another approach - crystallization from bicelles - was proposed. This method was first applied to obtain well diffracting bR crystals [18,19]. Bicelles, known for quite a long time, are a liquid crystal phase consisting of disc-shaped lipid-rich bilayer particles formed from mixtures of dimyristoyl phosphatidylcholine (DMPC) with certain detergents. The detergents mostly used for such a type of crystallization are either dihexanoyl phosphatidylcholine (DHPC) or zwitterionic bile salt derivative, CHAPSO. The bicelle sizes at a 1:3 DMPC/DHPC molar ratio are: the bilayer thickness - 40 \AA and the diameter - 400 \AA . The lipid detergent ratios present in the bicellar systems are relatively high compared to standard micellar systems [20,21].

The procedure of crystallization of membrane proteins from bicelles is as follows. The first step is preparation of bicelles. Then, solubilized protein is mixed with bicelles. It is considered, but not directly proven, that at this stage, the protein molecules are reconstituted into bicelles. After that the protein is crystallized by a standard vapor diffusion method. bR crystals grown at room temperature are identical to the previously obtained at 37°C twinned crystals: space group $P2_1$ (2.0 Å resolution) with unit cell dimensions of $a = 44.7$ Å, $b = 108.7$ Å, $c = 55.8$ Å, $\beta = 113.6^\circ$. The other room-temperature crystals were not-twinned and belong to space group $C222_1$ (2.2 Å resolution) with the following unit cell dimensions: $a = 44.7$ Å, $b = 102.5$ Å, $c = 128.2$ Å. It is important to note that the crystals of the human β_2 -adrenergic GPCR were obtained by this method [22]. The structure was solved to 3.5/3.7 Å resolution. It is considerably lower than what was obtained by protein crystallization in the cubic phase [23]. Taking into account the long and dramatic attempts to crystallize a ligand binding GPCR, there is no doubt it was a new considerable success of the method under discussion. The 2.3 Å resolution structure of the murine voltage dependent anion channel (mVDAC) that reveals a high-resolution presentation of membrane protein architecture was also obtained due to bicelles method [24]. Very recent success of the bicelle-like approach is the crystallization of the membrane part of the respiratory complex I [25].

2.4 Crystallization from sponge phases (L_3 -phase)

It is interesting that historically crystallization from the sponge phase was described about 10 years after discovering the LCP approach. This is despite the fact that the sponge phase (L_3 -phase) is the liquid analogue of the lipidic cubic phase with the reduced bending rigidity of membranes and without a long-range order. When the bending rigidity of the membrane becomes comparable with a thermal energy the ordered cubic phase structure is perturbed by thermally excited collective out-of-plane fluctuations of membranes. The transformation of the cubic to the sponge phase can be induced by different factors, for instance, via adding a solvent such as polyethyleneglycol (Mw = 400), dimethyl sulfoxide, 2-methyl-2,4-pentanediol (MPD), propylene glycol, or Jeffamine M600 to a lipid/ water system [26]. The diameter of aqueous pores in the MO cubic phase is relatively narrow (ca. 3-6 nm) compared to that of the sponge phase (10-15 nm and more) [27]. Evidently the size of the pores of the L_3 -phase is compatible with membrane proteins with large hydrophilic parts and lets them diffuse freely within the plane of the membrane surface [26]. Well diffracting crystals of the reaction center from *Rhodobactersphaeroides* were grown in the L_3 by a conventional hanging-drop scheme of the experiment, and were harvested directly without the addition of lipase or cryoprotectant, and the structure was refined to 2.2 Å resolution. The authors of the work claimed that in contrast to the earlier LCP reaction center structure [28], the mobile ubiquinone could be built and refined. In these experiments, the only additional component (relative to the components of the cubic phase crystallization - the MO/membrane protein/detergent/buffer) was a small amphiphilic molecule 1,2,3-heptanetriol or Jeffamine M600. The structure was solved to resolution 2.35 Å [28]. In another work [29], crystals of the light harvesting II complex suitable for X-ray crystallography were obtained with structural 2.45 Å resolution. In this study, the additives used were KSCN, butanediol, pentaerythritolpropoxylate (PPO), *t*-butanol, Jeffamine, and 2-methyl-2,4-pentanediol (MPD). An advantage of the L_3 approach is that the liquid properties of the sponge phase at room temperature can be used directly in hanging- or sitting-drop vapor-diffusion

crystallization by commercially available robots. Recently, a sponge phase sparse matrix crystallization screen consisting of different conditions became available [30]. However, unlike the LCP method, this one has not led to a breakthrough in structural biology of membrane protein. There was no structure of a new membrane protein or a principal improvement in structural resolution achieved by this method. Does it mean that the sponge phase approach does not have the same (or higher) power as the LCP method? We would speculate that this approach can be at least considered as a complementary one to the LCP.

3. Overcoming twinning formation

3.1 Introduction to the merohedral twinning of bR P6₃ crystals

Although bR can be crystallized by many methods and in different types of symmetries [5,16,18,31], only P6₃ crystal grown by *in meso* crystallization diffracts to the highest resolution. At the same time, these crystals often suffer from perfect merohedral twinning [32].

Twinning is one of the most common crystalline defects. A twin crystal consists of several domains oriented in such a way that their reciprocal lattices are superimposed at least in one dimension [33]. There are two forms of twinning: merohedral and non-merohedral. Only part of reflections of individual crystal domains superimpose in non-merohedral twinning, whereas all reflections are superimposed in three space dimensions in the merohedral form [34]. If only two orientations of twin domains are present the merohedral twinning is called hemihedral. It is the most widespread type of merohedral twinning [33]. The hemihedral twinning is intrinsic for hexagonal P6₃ crystals of bR grown in the cubic phase of MO [32,35].

Twinning of bR crystals implies the imposition of reflections with Miller indexes hkl and $kh-l$, so that the observed crystal reflections is a weighted sum of two different crystallographic reflections:

$$\begin{aligned} I_{hkl}^{obs} &= (1-\alpha)I_{hkl} + \alpha I_{kh-l} \\ I_{kh-l}^{obs} &= (1-\alpha)I_{kh-l} + \alpha I_{hkl} \end{aligned} \quad (1)$$

Where I_{hkl}^{obs} are crystallographic intensities observed in the X-ray experiment, I_{hkl} are crystallographic intensities of the twin domains and α is the twinning ratio, i.e. the volume fraction of equally oriented domains. Twinning is called perfect when α is close to 50 %. The shape and optical properties of twinned crystals are identical to those without twinning. The presence of twinning and estimation of the twinning ration are only possible by using special analysis methods of the diffraction data [36].

Twinning of the crystals complicates the obtaining of a crystallographic structure of the protein. If the twinning ration is $\alpha \neq 50\%$, then the system (1) can be solved:

$$\begin{aligned} I_{hkl} &= \frac{(1-\alpha)I_{hkl}^{obs} - \alpha I_{kh-l}^{obs}}{1-2\alpha} \\ I_{kh-l} &= \frac{(1-\alpha)I_{kh-l}^{obs} - \alpha I_{hkl}^{obs}}{1-2\alpha} \end{aligned} \quad (2)$$

After that, the usual tools can be applied for crystallographic analysis. However, as follows from (2), the error in intensity calculation increases and tends to infinity as a tends to 50 % [37]. For this reason the presence of crystal twinning worsens the electron density maps and reduces the reliability of protein models.

The perfect hemihedral twinning of bR crystals shows up in the presence of additional two-fold symmetry since $I_{hkl}^{obs} = I_{kh-l}^{obs}$ (see (1) when $\alpha = 50\%$). In this case, the number of independent observations (crystallographic intensities) is two times fewer. The equation system (1) is confluent and the crystallographic intensities cannot be extracted from the X-ray data. In this case, the intensities calculated from the protein model are used to obtain the desired crystallographic intensities according to the equation:

$$I_{hkl} = \frac{I_{hkl}^{obs} + I_{hkl}^{cal} - I_{kh-l}^{cal}}{2} \quad (3)$$

$$I_{kh-l} = \frac{I_{hkl}^{obs} + I_{kh-l}^{cal} - I_{hkl}^{cal}}{2}$$

where I_{hkl}^{cal} are intensities calculated from the protein model. R-factors of protein models obtained from the perfect twinned data overestimate the model reliability, since the difference between the observed and calculated structural factors is undervalued due to the averaging over the reflections related by the twinning law. Hence, the refined crystallographic R-factors from perfectly twinned data are typically a factor of $1/\sqrt{2}$ lower than for low (or un-)twinned data [36,38,39]. In addition, the use for refinement of the intensities calculated according to (3) introduces additional model bias due to the explicit dependence of the detwinned data on the model itself.

An additional problem for X-ray analysis caused by perfect twinning is the inability to use the experimental difference Fourier map. Basing on the mathematical consideration it was shown about 40 years ago that the difference Fourier electron density maps are most sensitive, accurate and less susceptible to model bias method for observing limited structural changes [40]. The difference map is simply the Fourier transform of the amplitudes ($F_{exc} - F_{gr}$) (where F_{gr} and F_{exc} are the structural factors of the ground and excited state of the protein) and phases are taken from the model of the ground state. This type of maps visualizes the changes in the electron density between the first and second crystallographic datasets. If structural changes are visible at a reasonable significance level within a difference Fourier map, then it is a plausible feature of the experimental data. On the opposite side, if changes arise during crystallographic refinement and are not confirmed by the difference Fourier map, then they are probably artifacts. For this reason, the difference Fourier maps are the main criterion for detecting small structural changes in the macromolecular systems and were used in many studies, for instance: myoglobin-CO complex [41-44], photoactive yellow protein [45-48], sensory rhodopsin II [49] and bR [50-57]. In the case of perfect twinning of protein crystals, structural factors F_{gr} and F_{exc} cannot be obtained, and Fourier difference maps cannot be constructed.

Despite the fact that twinning creates problems for protein crystallography, currently there are no rational effective methods of obtaining untwinned crystals. Similarly there are only a few works published on the systematic study of interrelation between twinning formation and crystallization conditions. Description of the phenomenon of twinning is even poorer for the crystals of membrane proteins and particularly for those obtained by *in meso* crystallization.

However, the twinning problem is of particular importance for the case of bR. Among 28 bR structures obtained from $P6_3$ crystals, 19 are from crystals with perfect twinning [32]. The best resolution of bR crystallographic model is 1.43 Å [58]. However, all the structures with the resolution better than 1.9 Å were obtained from crystals with perfect twinning. The only exception is the structure with a resolution 1.55 Å from the crystal with a twinning ratio of 25 %. All the currently published crystallographic studies devoted to the K, L and M bR intermediate states either have a relatively low resolution (> 2.1 Å) [50-56] or were obtained from perfectly twinned crystals [58-63]. The intermediate state structures built using these data are not consistent with each other [53,56,64]. One of the most probable reasons for this is the twinning problem.

It is well known that the changes in bR structure during the transition from the ground state to intermediates are relatively small [50-55,58,60,62]. Thus, X-ray data of very high quality are required to obtain the structures of intermediate states. In particular, crystals should be untwinned as twinning reduces the quality of the electron density maps and the reliability of protein models, as well as suppresses the utilization of the Fourier difference maps. To elucidate the molecular mechanism of bR proton transport, it is crucial to obtain highly ordered crystals without twinning.

3.2 Physical detwinning of bR crystals

In 2004 [35] it was shown that the twinned crystals of bR consist of large scale domains. Each of the domains is a hexagonal plate with the size in the hexagonal plane equal to that of the whole crystal and the thickness comparable to that of the crystal (as it is shown in Fig.2). In most cases the crystals were split in two plates with no twinning. However in some cases the crystals were split in three and more plates. Thus it may be supposed that most of bR $P6_3$ crystals consist of only two twinning domains. However the presence of three and even more domains is also possible. But the size of these domains is always comparable to the size of the twinned crystal. The attempts to mechanically separate the twin domains had no effect. However it was noted that the slow decrease of mother liquid molarity may result in crystal slicing. Basing on this idea the approach for physical detwinning of bR crystals was proposed. According to the procedure the molarity of salt in mother liquid was slowly reduced from 3 to 1 M which induces splitting of agglutinated plates. Some of the split crystals diffracted well enough to determine the twin ratio which in all cases was equal to zero within the experimental error.

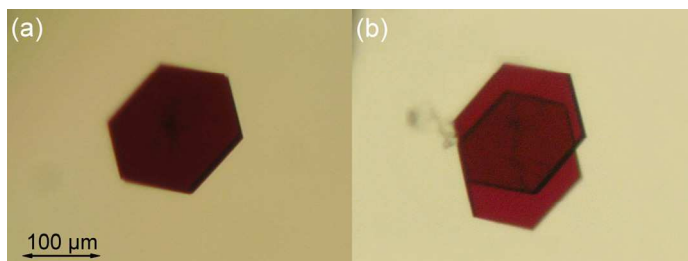


Fig. 2. bR crystal splits into two parts: (a) initial crystal, (b) two parts of the crystal separated by gradual decrease of the salt concentration.

Unfortunately, it turned out that the procedure of physical separation of the crystals often leads to a significant drop in the diffraction quality of the crystals, and therefore is not applicable in practice for obtaining high-resolution X-ray analysis.

3.3 Direct observation of twin domains

As it was mentioned before the twinning fraction of the crystal can only be estimated by the analysis of the statistical distribution of its crystallographic intensities. This implies that to determine the twinning, one has to fulfill the whole procedure of obtaining the crystallographic data, including the dissolution of the crystallographic sample, the separation of crystals from the crystallization matrix and X-ray data collection. Meanwhile, this resource- and time-consuming procedure has a small useful output: nine out of ten crystals have the twinning ratio close to 50 %.

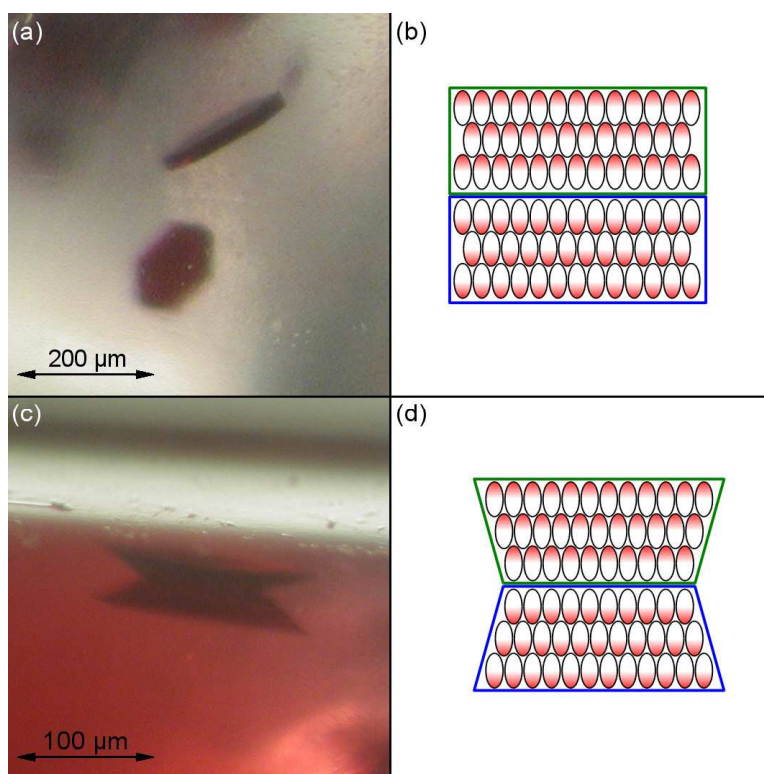


Fig. 3. bR crystals usually obtained by *in meso* crystallization in OG (a) and their schematic representation (b). bR crystals obtained by *in meso* crystallization in CYMAL-5 (c) with their schematic representation (d). Two different twin domains are shown in blue and green color. Red color represents the negative charge of CP side of bR.

One of the ways to simplify this procedure was found during crystallization trials with different detergent types [32]. It was observed that the crystals grown in the presence of 5-cyclohexyl-1-pentyl- β -D-maltoside (CYMAL-5) at concentrations of about 10 % have a shape of two truncated pyramids stuck together along the smaller of the hexagonal sides (Figure 3 c). Crystals in one crystallization probe had all the possible values of relative volumes of domains (from 0 when one domain was missing; to 0.5 when the domains had equal volume). The twinning ratio was surprisingly correlated with the relative domain volumes, which was confirmed by statistical analysis of X-ray intensities. The twinning fraction was close to 0 % when one of the domains was much smaller than the other, and close to 50 % for crystals with approximately equal parts. In addition, some of the crystals were split in two parts during fishing. Each of the domains had no twinning. Thus, it was concluded that the truncated pyramids represent twin domains as shown at Fig.3d. It is possible to select non-twinned crystals by careful inspection of the crystals shape in stereomicroscope, which significantly reduces the time and resources on the procedure for selection of crystals suitable for X-ray diffraction studies and produces additional information about the nature of the twinning formation.

3.4 Interrelation of crystal growth rate and twinning fraction

Additional information on the nature of bR twinning came from the statistical distribution of twinning ratio among several hundreds of crystals [32]. For this purpose bR crystals were grown in a wide range of crystallization conditions: at different concentrations of salt and protein, types and concentrations of detergents. More than 300 crystals were obtained and X-ray data were collected from all of them to determine their twinning ratios.

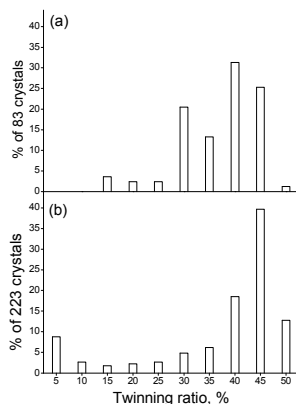


Fig. 4. Distribution of twinning ratios in two groups of crystals with the characteristic growth time less than 1.5 months (empty columns) (a) and more than 1.5 months (hatched columns) (b). The first and second groups consist of 83 and 227 crystals, respectively.

It turns out that regardless of the specific crystallization conditions the crystals with low twinning ratio (< 20 %) were observed with higher probability in samples where the first crystals appeared relatively late (in 2-3 weeks after sample preparation, rather than 2-3 days) and growth proceeds for a longer time period (for ~10 weeks). If the first crystals appeared in the sample relatively early and their growth was rapid then almost all crystals

had a high twinning ratio. The distribution of twinning ratio for 83 crystals grown less than 1.5 months and for 227 crystal with growth time of more than 1.5 months is shown at Figure 4. 11 % of the slowly grown crystals had the twinning ratio smaller than 10 %. Meanwhile all the fast grown crystals had the twinning ratio higher than 10 % and only 5 % had the twinning ratios between 10 % and 20 %.

It was suggested before for the soluble protein plastocyanin that slow growth favors the formation of untwinned crystals [39]. Confirmation of this relationship for a membrane protein, probably indicates the general nature of this phenomenon. It is plausible that in all cases when protein crystals suffer from twinning, one should search for the crystallization conditions of slow crystal growth.

3.5 Crystallisation in β -XyIOC₁₆₊₄ mesophase

A presumably new approach to obtaining non-twinned bR crystals unexpectedly comes from the *in meso* crystallization in the "exotic" β -XyIOC₁₆₊₄ mesophase.

The crystallization trials with this lipid were excited by the inequality of lipid and detergent libraries used for handling membrane proteins. The library of detergents with different hydrophilic and hydrophobic parts used for solubilization, purification and crystallization of membrane proteins is quite large. The fittest detergent may be found in the library for each specific membrane protein. On the contrary the library of lipids used for the cubic phase creation is discouragingly small. MO is the most common lipid for *in meso* crystallization. Three other monoglycerols are reported to be suitable for this type of crystallization: monopalmitolein [5], monovaccenin [66], 2,3-dihydroxypropyl-(7Z)-hexadec-7-enoate [67] and 2,3-dihydroxypropyl-(7Z)-tetradec-7-enoate [68]. The library of matrix lipids for *in meso* crystallization should be increased for further success of the method.

Recently we presented the results of bR crystallization in the β -XyIOC₁₆₊₄ cubic phase used for this purpose for the first time. β -XyIOC₁₆₊₄ (Fig.2 in [69]) represents a recently developed isoprenoid-chained lipid family [70,71].

β -XyIOC₁₆₊₄ forms a cubic phase almost at the same conditions as MO. It turns to be possible to crystallize bR in the β -XyIOC₁₆₊₄ cubic phase using the standard protocol of *in meso* crystallization [69]. Several dozens of crystals were obtained. Three of them diffracted well enough and the X-ray dataset was collected for them. Two crystals diffracted up to 2 Å . The third one was worse and gave diffraction up to 2.7 Å .

The crystals obtained in the cubic phase of β -XyIOC₁₆₊₄ and MO have the same P₆₃ symmetry. The diffraction quality of bR crystals obtained in β -XyIOC₁₆₊₄ is better than that of the first bR crystals obtained in MO [72] (the resolution is 2.0 Å and 2.5 Å, correspondingly). A further search for optimal crystallization conditions will possibly improve the diffraction properties as it was done in the case of MO.

It is important to mention that three studied crystals had a low twinning ratio. The twinning ratio was 37 and 34 % in two cases (for the crystals with diffraction resolution of 2.0 Å), and the third crystal (with resolution of 2.7 Å) had no twinning. As follows from §3.4 and [32], only 28 % of crystals obtained in the MO cubic phase have the twinning ratio smaller than 34 %. Thus the probability to find in one crystallization probe three crystals with small twinning ratios is relatively low which is unlikely to be a coincidence. The β -XyIOC₁₆₊₄ cubic phase may favor the formation of low-twinned crystals.

3.6 The nature of the twinning phenomenon

Experiments described in 3.2-3.5 gave enough information to produce untwinned bR crystals for the investigation of the proton transport mechanism. On the other hand they gave some hints to understand the nature of the phenomenon of twinning formation in bR crystal.

bR crystals belong to class I in the nomenclature introduced in [73]. The hexagonal plane of bR crystals is perpendicular to the crystallographic axis c which implies that crystal growth occurs through layer-by-layer two-dimensional nucleation on the ab surfaces of the crystal [74]. This assumption is in accordance with the model of *in meso* crystal growth proposed by M. Caffrey [75] and is confirmed by atomic force microscopy [76]. The contact surface between twinning domains is also perpendicular to c axis as it is demonstrated in Fig.3. Consequently, this surface also emerges as a result of two-dimensional nucleation on the ab -surface.

The contact surface may be formed either by two cytoplasmic (CP) surfaces of bR or two extracellular (EC) ones. The twinning ratio of the majority of crystals is $> 30\%$, and most of them consist of two domains. This peculiarity may be explained by different energies of interaction for CS-CS and EC-EC contacts in the protein crystal. As follows from the pdb-structure (1C3W [77] for instance) EC surface of bR is almost neutral and CP is negatively charged. On the other hand there is no specific interaction seen in pdb-structures between two adjacent protein layers, they interact by Van-der-Waals contacts between only two amino acids [72]. That means that even a weak electrostatic interaction may play an important role in the total energy of layer interaction.

Thus we can imagine the following process of crystal formation: the first twin domain emerges soon after (or even during) nucleation with two twin domains interacting by their EC surfaces. The crystal itself has two CP surfaces at its external faces. The probability to form a new twin domain on the CP surface is relatively low due to unfavourable electrostatic interaction. Consequently, the crystal continues to grow without formation of new twinning domains.

It may be noted that the distribution of the twinning fraction of slowly growing crystals has a sinuous pattern: there are local maxima with the twinning ratio $< 10\%$ and $> 35\%$, and a minimum is located in between them. This non-obvious behavior may be explained by computer modelling of the growth of twin crystals.

As it was mentioned before crystal growth occurs through the two-dimensional nucleation at the surface of the crystal (slow step) and a relatively fast growth of the new layer in two dimensions. Thus one can use a one-dimensional model to simulate crystal growth in the direction perpendicular to the ab crystallographic plane. Crystal growth begins from a single layer and proceeds by consecutive addition of new layers to each surface of the crystal alternatively. When a new layer is added three different types of contacts may be formed.

1. CP-EC contacts which corresponds to normal crystal growth. Let us assign to this event a relative probability of 1.
2. EC-EC contacts which corresponds to the formation of the twinning domain. We will assign the probability P_1 to this event.
3. CP-CP contacts which also gives rise to a twinning domain as probability P_2 is assigned to this event.

The usual thickness of P6₃ bR crystal is about 20 μm that corresponds to about 4000 protein layers. This number of layers was used in the simulation of the crystal growth.

There are two variables which will dictate the number of formed twinning domains and the twinning ratio of the crystal: the probabilities P_1 and P_2 . These probabilities may be varied to fit the experimental dependencies shown at Fig.4.

The first feature noted while exploring this model was that the symmetrical conditions ($P_1 = P_2$) cannot reproduce the experimental data. Under relatively low probabilities of twinning formation the distribution shows a peak at zero twinning ratio. The height of the peak decreases as the probability of twin formation increases and the distribution over the nonzero range remains quite flat until the peak at zero vanishes (Fig. 5a).

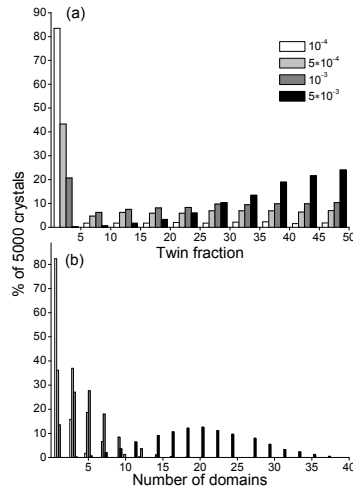


Fig. 5. Distribution of twinning fraction (a) and (b) the number of twinning domains calculated for 5000 crystals under conditions of symmetric domain nucleation ($P_1=P_2$) and for probabilities in the range 10^{-4} - 5×10^{-3} .

When an asymmetry in the probabilities is introduced to the model with $P_1=10^{-3}$, the peak at zero value changes very little, while the rest of the distribution has low values at low twinning ratios which gradually increase towards higher twinning ratios (Fig. 6a). Two important things are worth noting here. Firstly, when P_2 is smaller than P_1 it has almost no influence on the distribution. P_2 is the probability of forming CP-CP. As it was described above this event is quite improbable because the two negatively charged CP surfaces are pushing apart. Thus P_2 can be fixed at 0 at the following consideration. Second, the introduction of asymmetry leads to a shift in the peak of the number of twin domains distribution (compare Fig. 5b and 6b) from six domains (for $P_1 = P_2 = 10^{-3}$) to two domains ($P_1 = 10^{-3}$, $P_2 = 0$) which is in accordance with the experimental results.

Under the asymmetrical conditions the model resembles the experimentally observed distributions. Small changes in P_1 lead to dramatic changes in the fractions of non-twinned and perfectly twinned crystals, while the fraction of crystals with an intermediate twinning ratio changes much more slowly. The best fit of the experimentally observed distributions corresponds to a probability P_1 of 3×10^{-3} for fast crystal growth, where less than 1 % of crystals grow without twinning, and of 1.25×10^{-3} for slow growth, where 10 % of crystals have no twinning (Fig.7).

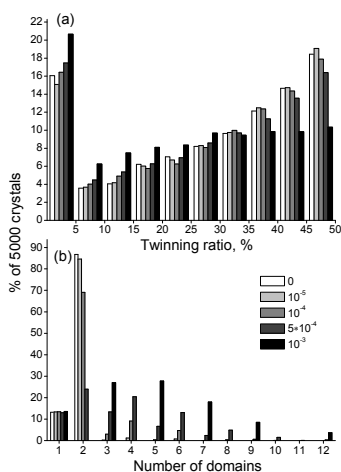


Fig. 6. Distribution of twinning ratio (a) and twinning domains (b) calculated for 5000 crystals under conditions of asymmetric domain nucleation $P_1=10^{-3}$, P_2 in the range between 0 and 10^{-3} .

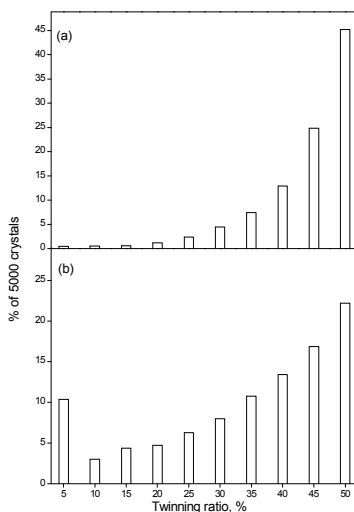


Fig. 7. Modelled distributions of twinning ratios simulating experimental distributions for slow (a) and fast (b) crystal growth. The P_1 probabilities for the models are 1.25×10^{-3} and 3×10^{-3} , correspondingly; $P_2 = 0$.

The model resembles the principal features of the experimentally observed distributions having quite a bad fit at the region of the high twinning ratio. This feature may be explained either by the underestimation of the twinning ratio by computational procedures owing to noise in the diffraction intensities or by the heterogeneity of the crystallization medium, which is responsible for the inevitable differences in the growth rates of different crystal surfaces.

The described model of twinning formation explains how the probabilities P_1 and P_2 determine the type of twinning fraction distribution. However, this model does not explain what is the relation between the rate of crystal growth and probabilities P_1 and P_2 . Unfortunately, the theory of *in meso* crystallization is quite poorly understood at the moment and it cannot be used to explain this dependence. However, we can imagine the following thermodynamic explanation:

The limiting step of the crystal growth is the two-dimensional nucleation on the crystal surface. According to the classical two-dimensional theory of crystallization the thermodynamic potential of nucleus formation is [78]:

$$\Delta G = -n(\mu_v - \mu_c) + \sum_i L_i \kappa_i \quad (4)$$

where μ_v and μ_c are chemical potentials of the protein molecule in the volume and on the crystal surface, n is the number of molecules in a nucleus. The second term describes the surface energy, where κ_i is a specific surface energy and L_i is the length of i -th edge.

Basing on (4) we can write down the general expression for the free energy:

$$\Delta G^* = -A\Delta\mu + B \quad (5)$$

where A and B are the values which are not dependent on $\Delta\mu = \mu_v - \mu_c$. A depends on the specific surface energy and is virtually equal for normal and twinning nucleation. B depends on the interaction of the molecules in different layers and is significantly different for normal and twinning nucleation.

The rate of two-dimensional nucleation represents as:

$$J \approx \Gamma e^{\frac{-\Delta G^*}{kT}} \quad (6)$$

where Γ poorly depends on $\Delta\mu$. The experimental fact that twinning domains have a macroscopic size results in the condition that the probability of normal layer nucleation is significantly higher than that of the twinning formation. Consequently:

$$J_0 \gg J_1; J_2 \Rightarrow \Delta G_0^* < \Delta G_1^*; \Delta G_2^* \quad (7)$$

where J_0 , J_1 and J_2 are the rates for normal and two twinning (CS-CS and EC-EC) nucleations, and ΔG_0^* , ΔG_1^* и ΔG_2^* are the corresponding free energies. The rate of crystal growth is regulated by supersaturation $\Delta\mu$ and at very high values of supersaturation the difference between J_0 , J_1 and J_2 vanishes (see (5)). When $\Delta\mu$ decreases, the absolute value of ΔG^* also diminishes and the growth rate drops down. As follows from (5), ΔG_1^* and ΔG_2^* approach 0 faster than ΔG_0^* and under a certain value of $\Delta\mu$ become positive (the formation of twin crystals ceases). Simultaneously, due to exponential dependency (6) the difference between probabilities of normal and twinning nucleations grows.

The described explanation is applicable for any crystals where twinning is formed by two-dimensional nucleation. For this type of crystals the correlation between the growth rate and the probability of twinning formation may be a common feature. Taking into consideration the presence of the lipidic cubic phase may give better understanding of the mechanism of the twinning formation.

The most important feature of the *in meso* crystallization mechanism for this consideration is the presence of lamellar lipid environment around the growing protein crystal (see Fig.1a in [75]). It is obvious that the highly curved transitional lipid phase should be present between the bulky cubic and lamellar phases. The changes in the cubic phase curvature will simultaneously cause the corresponding changes in the curvature of the transitional phase.

It was proposed in [79] that the protein *in meso* crystallization is provoked by excess of elastic energy in the curved lipid bilayer. This type of energy is accumulated by the crystallization system due to hydrophilic-hydrophobic mismatch between the lipid bilayer and the protein molecule and the value of this energy is strongly dependent on the bilayer curvature radius and the length of protein hydrophobic-hydrophilic boarder. The rate of crystal growth is regulated through the changes of the elastic energy caused by variations in the bilayer curvature. The decrease of the curvature radius results in the slowdown of crystal growth.

On the other hand the variations in the length of the hydrophilic-hydrophobic boarder also influence the crystallization rate. There are two substantially different hydrophilic-hydrophobic boarders of the protein molecule (one is at the EC side of the protein and the other is at the CP one). The curved bilayer is also asymmetrical relative to the perpendicular to its surface. Consequently, the elastic energy of deformation is dependent on the orientation of the protein in the curved bilayer.

The protein molecule has to cross the highly curved transitional bilayer during the crystallization and the corresponding energy barrier of this process is different for different orientations of protein molecules. And the character of the elastic energy dependence on the bilayer curvature is also different for the two possible protein orientations.

The decrease of the bilayer curvature during crystallization results in a slowdown of crystal growth and simultaneously reduces the curvature of the transitional region. The energy barriers for two different protein orientations change differently and this fact results in different probabilities of the formation of the normal or twinned protein layer in the crystal.

4. Conclusions

Twinning of protein crystals is an unwelcome phenomenon for crystallographers and may be a barrier, like in the case of bR crystals, on the way to elucidating protein function. For this reason the efforts were applied to understand and overcome it. Nowadays the twinning of bR P6₃ crystals is one of the most studied and characterised twinning phenomena of protein crystals.

First of all it was directly shown that the LCP grown twinned crystals of bR consist of large scale domains. Each of the domains is a hexagonal plate with the size equal to that of the whole crystal [35]. It is important the crystals may be split into several non-twinned domains by slow changes of salt concentration in the mother liquid so that the split parts preserved high diffraction quality. Further systematic investigation showed that the rate of crystal growth strongly affects the twinning-ratio distribution of the crystals. Searching for crystallization conditions leading to slow crystal growth, it is possible to select crystallization trials that contained up to 10% non-twinned crystals [32]. In addition, the conditions were found allowing selection of crystals with low twinning by visual inspection of their shape with no need for analysis of the diffraction intensity distribution. This discovery further facilitates the process of selection of non-twinned crystals. The experimental data obtained so far allow the formulation of a theory of twinning formation

which in particular sheds some light on the general question of the process of *in meso* crystallization. Most recently some hints were found that the usage of different crystallization matrixes may allow to improve the yield of non-twinned crystals in crystallization [69].

5. Acknowledgements

Authors are grateful to Georg Büldt, Rouslan Efremov and Ekaterina Round for their contribution to the chapter. Authors are supported by the program "Chairesd'excellence" édition 2008 of ANR France, CEA(IFS)-HGF(FZJ) STC 5.1 specific agreement, the German Federal Ministry for Education and Research (PhoNa - Photonic Nanomaterials), the MC grant for training and career development of researchers (Marie Curie, FP7-PEOPLE-2007-1-1-ITN, project SBMPs), an EC FP7 grant for the EDICT consortium (HEALTH-201924), Russian State Contracts No. 02.740.11.0299, 02.740.11.5010, P974 of activity 1.2.2, and No. P211 of activity 1.3.2 of the Federal Target Program "Scientific and Academic Research Cadres of Innovative Russia" for 2009–2013.

6. References

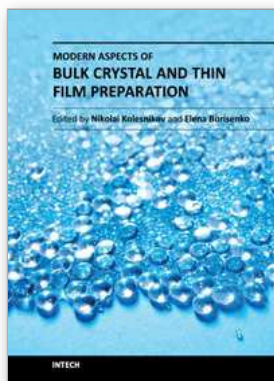
- [1] Deisenhofer J. et al., Structure of the protein subunits in the photosynthetic reaction centre of *Rhodospseudomonas viridis* at 3[angst] resolution, *Nature* 318 (1985) 618-624.
- [2] White S.H., The progress of membrane protein structure determination, *Protein Sci.* 13 (2004) 1948-1949.
- [3] The Protein Data Bank, <http://www.pdb.org/> (2011)
- [4] Hirai T. et al., Structural snapshots of conformational changes in a seven-helix membrane protein: lessons from bacteriorhodopsin, *Current Opinion in Structural Biology* 19 (2009) 433-439.
- [5] Landau E.M. et Rosenbusch J.P., Lipidic cubic phases: A novel concept for the crystallization of membrane proteins, *Proc.Natl.Acad.Sci.USA* 93 (1996) 14532-14535.
- [6] Mariani P. et al., Cubic phases of lipid-containing systems. Structure analysis and biological implications, *J.Mol.Biol.* 204 (1988) 165-189.
- [7] Luzzati V. et al., Structure of the cubic phases of lipid-water systems, *Nature* 220 (1968) 485-488.
- [8] Scriven L.E., Equilibrium Bicontinuous Structure, *Nature* 263 (1976) 123-125.
- [9] Landh T., From entangled membranes to eclectic morphologies: cubic membranes as subcellular space organizers, *FEBS Lett.* 369 (1995) 13-17.
- [10] Fontell K., Cubic phases in surfactant and surfactant-like lipid systems, *Colloid & Polymer Science* 268 (1990) 264-285.
- [11] B.Ericsson et al., Cubic Phases as Delivery Systems for Peptide Drugs, в: *Polymeric Drugs and Drug Delivery Systems*, American Chemical Society, (1991) 251-265.
- [12] V.I.Gordeliy et al., Crystallization in lipidic cubic phases: A case study with Bacteriorhodopsin, *Membrane Protein Protocols: Expression, Purification, and Crystallization*, ed. B.Selinsky, publ.: Humana Press, Totowa NJ, (2003) 305-316.
- [13] Caffrey M. et Cherezov V., Crystallizing membrane proteins using lipidic mesophases, *Nature Protocols* 4 (2009) 706-731.

- [14] Nollert P. et Landau E.M., Enzymic release of crystals from lipidic cubic phases, *Biochem.Soc.Trans.* 26 (1998) 709-713.
- [15] Kouyama T. et al., Polyhedral assembly of a membrane protein in its three-dimensional crystal, *J.Mol.Biol.* 236 (1994) 990-994.
- [16] Takeda K. et al., A novel three-dimensional crystal of bacteriorhodopsin obtained by successive fusion of the vesicular assemblies, *J.Mol.Biol.* 283 (1998) 463-474.
- [17] Denkov N.D. et al., Electron cryomicroscopy of bacteriorhodopsin vesicles: mechanism of vesicle formation, *Biophys.J.* 74 (1998) 1409-1420.
- [18] Faham S. et Bowie J.U., Bicelle crystallization: a new method for crystallizing membrane proteins yields a monomeric bacteriorhodopsin structure, *J.Mol.Biol.* 316 (2002) 1-6.
- [19] Faham S. et al., Crystallization of bacteriorhodopsin from bicelle formulations at room temperature, *Protein Sci.* 14 (2005) 836-840.
- [20] Sanders C.R. et Schwonek J.P., Characterization of magnetically orientable bilayers in mixtures of dihexanoylphosphatidylcholine and dimyristoylphosphatidylcholine by solid-state NMR, *Biochemistry* 31 (1992) 8898-8905.
- [21] Sanders C.R. et Prestegard J.H., Magnetically orientable phospholipid bilayers containing small amounts of a bile salt analogue, CHAPSO, *Biophys.J.* 58 (1990) 447-460.
- [22] Rasmussen S.G. et al., Crystal structure of the human beta2 adrenergic G-protein-coupled receptor, *Nature* 450 (2007) 383-387.
- [23] Cherezov V. et al., High-resolution crystal structure of an engineered human beta2-adrenergic G protein-coupled receptor, *Science* 318 (2007) 1258-1265.
- [24] Ujwal R. et al., The crystal structure of mouse VDAC1 at 2.3 Å resolution reveals mechanistic insights into metabolite gating, *Proc.Natl.Acad.Sci.U.S.A* 105 (2008) 17742-17747.
- [25] Efremov R.G. et al., The architecture of respiratory complex I, *Nature* 465 (2010) 441-445.
- [26] S.Engstrom et al., Solvent-induced sponge (L3) phases in the solvent-monoolein-water system, *The Colloid Science of Lipids*, ed. B.Lindman, B.Ninham, publ.: Springer Berlin / Heidelberg, 1998) 93-98.
- [27] Ridell A. et al., On the water content of the solvent/monoolein/water sponge (L3) phase, *Colloids and Surfaces A: Physicochemical and Engineering Aspects* 228 (2003) 17-24.
- [28] Katona G. et al., Lipidic cubic phase crystal structure of the photosynthetic reaction centre from *Rhodobacter sphaeroides* at 2.35Å resolution, *J.Mol.Biol.* 331 (2003) 681-692.
- [29] Cherezov V. et al., Room to move: crystallizing membrane proteins in swollen lipidic mesophases, *J.Mol.Biol.* 357 (2006) 1605-1618.
- [30] Wohri A.B. et al., A lipidic-sponge phase screen for membrane protein crystallization, *Structure.* 16 (2008) 1003-1009.
- [31] Schertler G.F. et al., Orthorhombic crystal form of bacteriorhodopsin nucleated on benzamidine diffracting to 3.6 Å resolution, *J.Mol.Biol.* 234 (1993) 156-164.
- [32] Borshchevskiy V. et al., Overcoming merohedral twinning in crystals of bacteriorhodopsin grown in lipidic mesophase, *Acta Crystallogr.D.Biol.Crystallogr.* 66 (2010) 26-32.
- [33] Parsons S., Introduction to twinning, *Acta Crystallogr.D Biol.Crystallogr.* 59 (2003) 1995-2003.

- [34] Dauter Z., Twinned crystals and anomalous phasing, *Acta Cryst. D* 59 (2003) 2004-2016.
- [35] Efremov R. et al., Physical detwinning of hemihedrally twinned hexagonal crystals of bacteriorhodopsin, *Biophys.J.* 87 (2004) 3608-3613.
- [36] Yeates T.O., Detecting and overcoming crystal twinning, *Methods Enzymol.* 276 (1997) 344-358.
- [37] Royant A. et al., Detection and characterization of merohedral twinning in two protein crystals: bacteriorhodopsin and p67(phox), *Acta Crystallogr.D Biol.Crystallogr.* 58 (2002) 784-791.
- [38] Royant A. et al., Detection and characterization of merohedral twinning in two protein crystals: bacteriorhodopsin and p67(phox), *Acta Crystallogr.D Biol.Crystallogr.* 58 (2002) 784-791.
- [39] Redinbo M.R. et al., The 1.5-Å crystal structure of plastocyanin from the green alga *Chlamydomonas reinhardtii*, *Biochemistry* 32 (1993) 10560-10567.
- [40] Henderson R. et Moffat J.K., The difference Fourier technique in protein crystallography: errors and their treatment, *Acta Cryst. B* 27 (1971) 1414-1420.
- [41] Schlichting I. et al., Crystal-Structure of Photolyzed Carbonmonoxy-Myoglobin, *Nature* 371 (1994) 808-812.
- [42] Srajer V. et al., Photolysis of the carbon monoxide complex of myoglobin: nanosecond time-resolved crystallography, *Science* 274 (1996) 1726-1729.
- [43] Srajer V. et al., Protein conformational relaxation and ligand migration in myoglobin: a nanosecond to millisecond molecular movie from time-resolved Laue X-ray diffraction, *Biochemistry* 40 (2001) 13802-13815.
- [44] Schotte F. et al., Watching a protein as it functions with 150-ps time-resolved x-ray crystallography, *Science* 300 (2003) 1944-1947.
- [45] Genick U.K. et al., Structure of a protein photocycle intermediate by millisecond time-resolved crystallography, *Science* 275 (1997) 1471-1475.
- [46] Genick U.K. et al., Structure at 0.85 Å resolution of an early protein photocycle intermediate, *Nature* 392 (1998) 206-209.
- [47] Perman B. et al., Energy transduction on the nanosecond time scale: early structural events in a xanthopsin photocycle, *Science* 279 (1998) 1946-1950.
- [48] Ren Z. et al., A molecular movie at 1.8 Å resolution displays the photocycle of photoactive yellow protein, a eubacterial blue-light receptor, from nanoseconds to seconds, *Biochemistry* 40 (2001) 13788-13801.
- [49] Moukhametzianov R. et al., Development of the signal in sensory rhodopsin and its transfer to the cognate transducer, *Nature* 440 (2006) 115-119.
- [50] Edman K. et al., High-resolution X-ray structure of an early intermediate in the bacteriorhodopsin photocycle, *Nature* 401 (1999) 822-826.
- [51] Sass H.J. et al., Structural alterations for proton translocation in the M state of wild-type bacteriorhodopsin, *Nature* 406 (2000) 649-653.
- [52] Royant A. et al., Helix deformation is coupled to vectorial proton transport in the photocycle of bacteriorhodopsin, *Nature* 406 (2000) 645-648.
- [53] Matsui Y. et al., Specific damage induced by X-ray radiation and structural changes in the primary photoreaction of bacteriorhodopsin, *J.Mol.Biol.* 324 (2002) 469-481.
- [54] Kouyama T. et al., Crystal structure of the L intermediate of bacteriorhodopsin: Evidence for vertical translocation of a water molecule during the proton pumping cycle, *J.Mol.Biol.* 335 (2004) 531-546.

- [55] Edman K. et al., Deformation of helix C in the low temperature L-intermediate of bacteriorhodopsin, *J.Biol.Chem.* 279 (2004) 2147-2158.
- [56] Takeda K. et al., Crystal structure of the M intermediate of bacteriorhodopsin: allosteric structural changes mediated by sliding movement of a transmembrane helix, *J.Mol.Biol.* 341 (2004) 1023-1037.
- [57] Yamamoto M. et al., Crystal structures of different substates of bacteriorhodopsin's M intermediate at various pH levels, *J.Mol.Biol.* 393 (2009) 559-573.
- [58] Schobert B. et al., Crystallographic structure of the K intermediate of bacteriorhodopsin: Conservation of free energy after photoisomerization of the retinal, *J.Mol.Biol.* 321 (2002) 715-726.
- [59] Lanyi J. et Schobert B., Crystallographic structure of the retinal and the protein after deprotonation of the Schiff base: the switch in the bacteriorhodopsin photocycle, *J.Mol.Biol.* 321 (2002) 727-737.
- [60] Lanyi J.K. et Schobert B., Mechanism of proton transport in bacteriorhodopsin from crystallographic structures of the K, L, M-1, M-2, and M-2' intermediates of the photocycle, *J.Mol.Biol.* 328 (2003) 439-450.
- [61] Schobert B. et al., Crystallographic structures of the M and N intermediates of bacteriorhodopsin: assembly of a hydrogen-bonded chain of water molecules between Asp-96 and the retinal Schiff base, *J.Mol.Biol.* 330 (2003) 553-570.
- [62] Lanyi J.K. et Schobert B., Structural changes in the L photointermediate of bacteriorhodopsin, *J.Mol.Biol.* 365 (2007) 1379-1392.
- [63] Facciotti M.T. et al., Structure of an early intermediate in the M-state phase of the bacteriorhodopsin photocycle, *Biophys.J.* 81 (2001) 3442-3455.
- [64] Lanyi J.K., What is the real crystallographic structure of the L photointermediate of bacteriorhodopsin?, *Biochim.Biophys.Acta* 1658 (2004) 14-22.
- [65] Seddon A.M. et al., Membrane proteins, lipids and detergents: not just a soap opera, *Biochim.Biophys.Acta* 1666 (2004) 105-117.
- [66] Gordeliy V.I. et al., Molecular basis of transmembrane signalling by sensory rhodopsin II-transducer complex, *Nature* 419 (2002) 484-487.
- [67] Misquitta Y. et al., Rational design of lipid for membrane protein crystallization, *J.Struct.Biol.* 148 (2004) 169-175.
- [68] Misquitta L.V. et al., Membrane protein crystallization in lipidic mesophases with tailored bilayers, *Structure.* 12 (2004) 2113-2124.
- [69] Borshchevskiy V. et al., Isoprenoid-chained lipid [beta]-XylOC16+4--A novel molecule for in meso membrane protein crystallization, *Journal of Crystal.Growth* 312 (2010) 3326-3330.
- [70] Yamashita J. et al., New lipid family that forms inverted cubic phases in equilibrium with excess water: molecular structure-aqueous phase structure relationship for lipids with 5,9,13,17-tetramethyloctadecyl and 5,9,13,17-tetramethyloctadecanoyl chains, *J.Phys.Chem.* B112 (2008) 12286-12296.
- [71] Hato M. et al., Aqueous phase behavior of lipids with isoprenoid type hydrophobic chains, *J.Phys.Chem.* B113 (2009) 10196-10209.
- [72] Pebay-Peyroula E. et al., X-ray structure of bacteriorhodopsin at 2.5 angstroms from microcrystals grown in lipidic cubic phases, *Science* 277 (1997) 1676-1681.
- [73] Michel H., *Crystallization of Membrane Proteins*, (1991)
- [74] McPherson A., *Crystallization of biological macromolecules*, (1999)

- [75] Caffrey M., Crystallizing membrane proteins for structure determination: use of lipidic mesophases, *Annu.Rev.Biophys.*38 (2009) 29-51.
- [76] Qutub Y. et al., Crystallization of transmembrane proteins in cubo: mechanisms of crystal growth and defect formation, *J.Mol.Biol.*343 (2004) 1243-1254.
- [77] Luecke H. et al., Structure of bacteriorhodopsin at 1.55 angstrom resolution, *J.Mol.Biol.*291 (1999) 899-911.
- [78] Markov I.V., Crystal growth for the begginers: Fundamentals of Nucleation, Crystal Growth and Epitaxy, second (2003)
- [79] Grabe M. et al., Protein interactions and membrane geometry, *Biophys.J.*84 (2003) 854-868.



Modern Aspects of Bulk Crystal and Thin Film Preparation

Edited by Dr. Nikolai Kolesnikov

ISBN 978-953-307-610-2

Hard cover, 608 pages

Publisher InTech

Published online 13, January, 2012

Published in print edition January, 2012

In modern research and development, materials manufacturing crystal growth is known as a way to solve a wide range of technological tasks in the fabrication of materials with preset properties. This book allows a reader to gain insight into selected aspects of the field, including growth of bulk inorganic crystals, preparation of thin films, low-dimensional structures, crystallization of proteins, and other organic compounds.

How to reference

In order to correctly reference this scholarly work, feel free to copy and paste the following:

V. Borshchevskiy and V. Gordeliy (2012). Crystallization of Membrane Proteins: Merohedral Twinning of Crystals, Modern Aspects of Bulk Crystal and Thin Film Preparation, Dr. Nikolai Kolesnikov (Ed.), ISBN: 978-953-307-610-2, InTech, Available from: <http://www.intechopen.com/books/modern-aspects-of-bulk-crystal-and-thin-film-preparation/crystallization-of-membrane-proteins-merohedral-twinning-of-crystals>

INTECH
open science | open minds

InTech Europe

University Campus STeP Ri
Slavka Krautzeka 83/A
51000 Rijeka, Croatia
Phone: +385 (51) 770 447
Fax: +385 (51) 686 166
www.intechopen.com

InTech China

Unit 405, Office Block, Hotel Equatorial Shanghai
No.65, Yan An Road (West), Shanghai, 200040, China
中国上海市延安西路65号上海国际贵都大饭店办公楼405单元
Phone: +86-21-62489820
Fax: +86-21-62489821

© 2012 The Author(s). Licensee IntechOpen. This is an open access article distributed under the terms of the [Creative Commons Attribution 3.0 License](#), which permits unrestricted use, distribution, and reproduction in any medium, provided the original work is properly cited.